comunicaciones técnicas

66

Vol. 9

1978 Serie Naranja: Investigaciones No. 175

THEORY OF CONNECTIVITY: APPLICATIONS TO SCATTERING OF SEISMIC WAVES. I. SH WAVE MOTION. *

F.J. Sabina**

I. Herrera ***

R. England**

*To appear in the proceedings of the Second International Conference on Microzonation, San Francisco, U.S.A. November 26-December 1, 1978.

**Investigador del IIMAS-UNAM.

***Investigador del IIMAS-UNAM y Asesor del Instituto de Ingeniería.

Recibida 19/VII/78

INSTITUTO DE INVESTIGACIONES EN MATEMATICAS APLICADAS Y EN SISTEMAS

UNIVERSIDAD NACIONAL AUTONOMA DE MEXICO

APARTADO POSTAL 20-726
MEXICO 20, D. F.
548-54-65

IIMAS UNAM

ABSTRACT

The purpose of this paper is to present a method, based on the Theory of Connectivity recently developed, to solve numerically the problem of scattering of seismic waves by bounded obstacles of arbitrary shape in an infinite domain, such as a canyon in a half-space. This method reduces the dimension of the problem by one but avoids the introduction of singular integral equations. The results obtained are compared with some known exact solutions for SH wave motion, producing very good agreement. Results for an irregular shaped obstacle are also given. It is observed that, in some cases of a trench with vertical walls, local amplification factors can significantly exceed 100%.

INTRODUCTION

In earthquake engineering and strong-motion seismology, the surface motion at a given site due to incoming seismic waves is of interest. For rough topography this problem may be approached as one of scattering and diffraction of elastic waves by departures from flatness. Owing to its mathematical complexity, it has not been completely solved. There are a few known exact solutions (26, 28). Also some approximate solutions have been obtained by regular (9, 16) and singular perturbations (18, 19). In these the wavelength is taken to be large compared with a characteristic linear dimension of the topography, which is not the case in the present study.

Thus numerical methods are sought for intermediate values of the wavelength. Finite difference (3, 4) and finite element methods (24) have been used with some success. However, when applied to unbounded regions, they use a bounded domain involving "artificial" boundaries that contaminate the solution. The effect may be reduced by considering a larger domain, but this may produce computer storage difficulties. On the other hand, the problem of eliminating the errors introduced by artificial boundaries has only been partially solved (23).

Alternatively, boundary integral equations have been employed for this problem (27). The integral equation has a singularity which must be handled with care. As other boundary methods, this procedure reduces the dimension of the space, but the solution is non-existent or non-unique at certain frequencies (8). In another representation (21), this difficulty is avoided but the equation is still singular.

Other methods have been used: an acoustic approximation valid for saturated soils (22); the discrete wave-number representation of Aki, Larner and Bouchon (1, 5, 6, 7); a collocation method (20). This last one produces an over-determined system of equations which is solved in terms of a generalized matrix inverse, but it also suffers from a lack of uniqueness at certain frequencies.

In this paper the solution of the problem of scattering of a plane harmonic SH wave incident upon a bounded reentrant rough topography in an otherwise flat, traction-free surface, is sought. In the method of solution, the scattered field is represented as a linear combination of known solutions of the wave equation. The coefficients are chosen to minimize the mean-square error in the boundary condition. The development of this approach has been guided by a theory of connectivity recently developed (10, 11), which allows a systematic formulation of boundary methods (12) applicable to many other problems and which leads naturally to the complete system of functions used here for the half-space (13). However, the corresponding system of functions for problems formulated in the whole space has been used extensively in the null-field method of acoustics and electromagnetism (2). Minimization of the mean-square error on the boundary is a standard technique (15), whose implications have not been fully realized until recently. In (17), it is shown that when the mean-square error is minimized on the boundary, the resulting representation converges uniformly to the solution of the problem provided a complete set of functions is chosen, as is the case in the present work.

The procedure here presented reduces the dimension by one without introducing singular integral equations. The theory of connectivity (10, 11, 13) also simplifies the treatment of the problem of scattering by bounded inhomogeneities such as an alluvial valley, as will be shown in another paper.

STATEMENT OF THE PROBLEM

Consider a two-dimensional half-space, y>0 (as in Fig. 1), consisting of

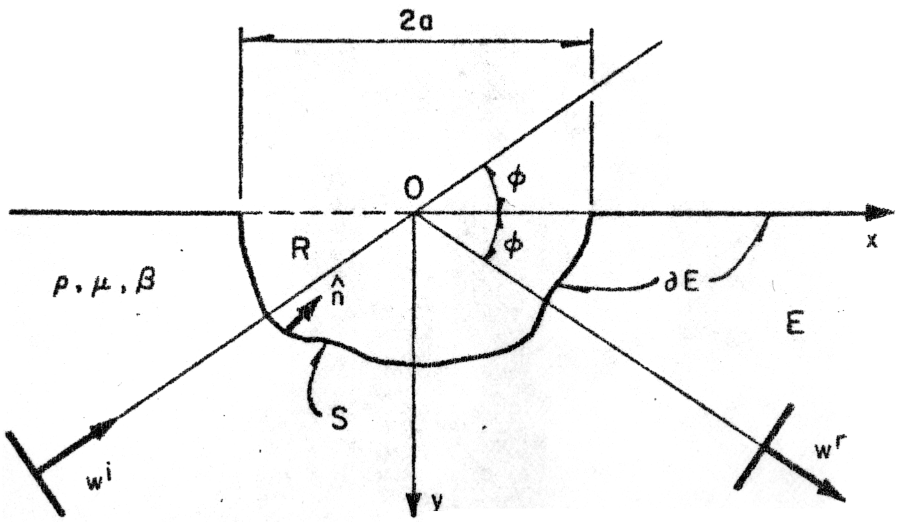

Figure 1. Illustrative topography.

two parts: an unbounded region E enclosing a bounded region R which contains the origin of coordinates 0. Let the boundary of E be ∂E and the common boundary between R and E be S. The surface S is assumed smooth in the sense of having continuously turning normal vector $\hat{n}$. The unbounded region E is filled with a linear elastic, homogeneous, isotropic medium of density ρ and rigidity μ; shear wave velocity is $\beta=(\rho/\mu)^{1/2}$. On the other hand, the bounded region R, having a characteristic horizontal linear dimension 2a, is empty. The surface ∂E is traction-free.

A state of antiplane shear deformation and harmonic motions in time is considered, so that the only non-zero component of the displacement is $w = w(x,y)\exp(i\omega t)$ in the z (out-of-plane) direction where ω is the circular frequency. Consider a plane harmonic SH wave w^i of unit amplitude incident upon R at an angle ϕ measured with respect to the x-axis (Fig. 1)

$$w^i = \exp[ik(-x\cos\phi + y\sin\phi)] \qquad [1]$$

with $k=\omega/\beta$. For convenience the factor $\exp(i\omega t)$ is omitted here and henceforth.

In the absence of the scattering region R, i.e. if the surface is flat, a reflected plane harmonic SH wave

$$w^r = \exp[-ik(x\cos\phi + y\sin\phi)] \qquad [2]$$

arises, so that a total field $w^o=w^i+w^r$ is produced in y>0.

In the presence of R, the scattered wave w produced by R is sought, such that the total field w^t may be written as

$$w^t = w^o + w \quad \text{in } E\ . \qquad [3]$$

Thus the scattered field satisfies the following boundary value problem

$$\nabla^2 w + k^2 w = 0 \quad \text{in } E\ , \quad \frac{\partial w}{\partial n} = -\frac{\partial w^o}{\partial n} \quad \text{on } \partial E\ , \qquad [4]$$

and w satisfies Sommerfeld's outward radiation condition at infinity, where $\nabla^2 \equiv \partial^2/\partial x^2 + \partial^2/\partial y^2$ is the Laplacian operator in two dimensions and $\partial/\partial n$ is the derivative in the direction of the outward unit normal $\hat{n}$ to ∂E. It may be observed that the right-hand side of Eq. [4b] is, in general, non-zero only on S, i.e. the common boundary between R and E.

Once w is found, the total field w^t can be determined. In strong-motion seismology it is of interest to find the surface field i.e. w^t on ∂E, and in particular, on S and close to it. A method for doing this is described here.

METHOD OF SOLUTION

Consider the complete system of cylindrical wave functions derived in a previous paper (13):

$$v_p = H_p^{(1)}(kr)\cos p\theta\ , \quad p = 0,1,2,\ldots \qquad [5]$$

where $H_p^{(1)}(z)$ is Hankel's function of the first kind of order p and (r,θ) are the polar coordinates of the point (x,y). Note that each v_p is a solution of Eq. [4a], fulfills $\partial v_p/\partial n = 0$ on y = 0, and satisfies a Sommerfeld outgoing radiation condition.

Let the N-th approximation to w be

$$w_N(r,\theta) = \sum_{p=0}^{N} a_p^N v_p(r,\theta) \quad , \qquad [6]$$

where the superindex N on the complex coefficients a_p^N has been introduced, to make explicit their dependence on the order of the approximation. In the work here reported, these coefficients were determined by minimizing the mean-square error on the boundary given as

$$\int_S \left| \frac{\partial w^o}{\partial n} + \frac{\partial w_N}{\partial n} \right|^2 ds \ . \qquad [7]$$

By a straightforward derivation, this procedure yields an (N+1)x(N+1) system of linear algebraic equations

$$B\underline{a} = \underline{c} \ , \qquad [8]$$

where the elements of the matrix B and the vector $\underline{c}$ are

$$b_{pq} = \int_S \frac{\partial \bar{v}_p}{\partial n} \frac{\partial v_q}{\partial n} ds \quad , \quad c_p = -\int_S \frac{\partial \bar{v}_p}{\partial n} \frac{\partial w^o}{\partial n} ds \ . \qquad [9]$$

The bar indicates a complex conjugate. The matrix $B=[b_{pq}]$ is Hèrmitian and positive definite; a numerically advantageous fact.

Since it is known that the set of functions $\{\partial v_p/\partial n\}$ is complete with respect to all functions that are square-integrable on S, $\partial w_N/\partial n$ converges uniformly in S to $\partial w/\partial n$. A proof in a very similar case is given in (17). Furthermore, $w_N(r,\theta)$ converges uniformly in E to the solution w of Eqs. [4].

Hence, for given N, the system of Eq. [8] is solved for the coefficients a_p^N, and finally Eq. [6] will produce the scattered field at any desired point in E, or, in particular on ∂E.

It is worthwhile observing that when S is a semicircle of radius a, the functions $H_p^{(1)}(kr)$ and their derivatives are constant on S, and the set of basis functions $\{v_p\}$ or $\{\partial v_p/\partial n\}$ is orthogonal on S in the sense that the matrix B is diagonal. The coefficients a_p^N are then independent of N, and Eq. [6] represents simply N+1 terms of the trigonometric Fourier series for w at any fixed value of r.

Since the displacement w is a complex function, it is necessary to calculate, as functions of the normalized abscissa x/a, its modulus and its phase

$$|w| = [(\mathrm{Re}\ w)^2 + (\mathrm{Im}\ w)^2]^{1/2} \quad , \quad \mathrm{ph}(w) = \tan^{-1}(\mathrm{Im}\ w/\mathrm{Re}\ w). \qquad [10]$$

The latter is arbitrarily divided by a normalizing factor 2π, mainly to facilitate comparison with other known solutions. In addition, the appropriate value of $\tan^{-1}$ is chosen to make ph(w) a continuous function, and a constant is subtracted to make its value zero at $x/a = 0$.

To deal with incident waves of different frequencies for fixed topography, a normalized frequency (or wave number) is introduced $\eta = \omega a/\pi\beta = ka/\pi$.

NUMERICAL CONSIDERATIONS

While evaluation of Eq. [7] would provide a criterion for the accuracy achieved, this has not so far been done. The simpler process of repeating the method for different values of N has been used: it is concluded that sufficient accuracy has been obtained when two solutions differ on S by less than the required error bound.

In addition to the value of N, it is necessary to fix some integration rule for the evaluation of Eqs. [9]. In view of the factor cos $p\theta$ in v_p, there are integrands in Eq. [9a] with up to N complete oscillations on S. Numerical experiments have given very poor results when the integration rule used fewer than 2N points, confirming a result from (29), reported in (17). Further, by varying the distribution of points, unsatisfactory results have been obtained with fewer than two integration points in each cycle of the factor $\cos^2(N\theta)$ in b_{NN}. This suggests the use of θ as the most suitable parameter in terms of which to write the equation of the curve S. A compound trapezoidal rule, with equal intervals in θ, clearly showed convergence to the correct values of a_p^N as the number of points increased above 2N. However, to obtain values of a_p^N with 1% accuracy, as many as 10N points were needed, using the trapezoidal rule with equal intervals in θ. Nevertheless, the same precision is attainable with fewer points using integration rules of higher order, provided the curve S, $r = r(\theta)$, is sufficiently smooth. In particular, with a compound 9 point Lobatto rule - coefficients from (25) - approximately 3N points were sufficient. A further increase in order did not appear productive, presumably because with increasing irregularity of the distribution of integration points, more than 3N points are required to maintain two in each cycle for $\cos^2(N\theta)$.

Having evaluated Eqs. [9], it remains to solve Eq. [8]. Since the matrix B is Hermitian and positive definite, an LU factorization without row interchanges should be possible, all the pivots being positive if rounding errors do not accumulate seriously. Further, it is possible to choose a Cholesky type factorization, $U = L^*$, the asterisk indicating the transposed complex conjugate, or to factorize B in the form LDL^*, where L is lower triangular with a unit diagonal, and D is real diagonal. This last form has in fact been used.

Probably the most costly part of the computation is the calculation of the Hankel functions $H_p^{(1)}(kr)$. These have been evaluated using Bessel function routines from the IBM Scientific Subroutine Package (14), slightly modified so as to provide values simultaneously for $p = 0, 1, \ldots, N$.

It should be noted that the matrix B does not depend upon the angle of incidence ϕ. Thus a considerable economy of computation is achieved if several angles of incidence are analysed simultaneously for a given geometry and wave number k.

RESULTS

In order to assess the method, a computer program using it has been applied to two cases with known exact solutions: semicylindrical (26) and semielliptical (28) canyons.

The solution for a semicylindrical canyon is given as a Fourier series with coefficients involving Bessel functions (26). The series was reevaluated numerically in the interval $|x/a| \leq 3$ for $\eta = 0.25\ (0.25)\ 2.0$ and angles of incidence $\phi = 0°\ (30)\ 90°$. Using the same number of terms for both methods (i.e. N = 19, 26, 33, 36, 38, 41, 43, 45 respectively), the modulus and phase of the displacement coincided in all the figures printed - a difference of less than 10^{-6}. Essentially the same precision could be achieved with fewer terms

For semielliptical canyons, the solution can be derived as a series involving Mathieu functions and the results are given in (28) as graphs of displacement amplitude and phase against normalized distance x/a from -3 to 3, with four angles of incidence 0°, 30°, 60°, 90°. Using the method of this article, semielliptical canyons of aspect ratio b = 0.7 have been analysed. (b = ratio of minor axis to major axis. For each value of b, there is both a shallow and a deep canyon). In the shallow case, using N = 22, 32, 36, 40 for η = 0.5, 1.0, 1.5, 2.0 respectively, the differences with (28) were in general less than 0.05 ~ 2.5% at $|x/a|$ = 0, 1, 2, 3, which is as good as the precision with which it is possible to read the graphs in (28). For η = 1.5, 2.0 no results were available for $|x/a|$ = 3. For η = 2.0, the differences were rather higher, rising as high as 0.25 at $|x/a|$ = 2, ϕ = 90°. Similar results were obtained for the deep case. Using the same values of N for η/b = 0.5, 1.0, 1.5, 2.0, differences were in general less than 0.05, at $|x/a|$ = 0, 1, 2, 3. For η/b = 2.0 no results were available for $|x/a|$ = 3, but the differences rose as high as 0.31 at $|x/a|$ = 2, ϕ = 0°.

However, by repeating the same cases with smaller values of N, successful convergence towards the solution was clearly observed. Estimated errors for the shallow canyon were less than 0.005 at $|x/a|$ = 0, 1, and 0.0005 at $|x/a|$ = 2,3 (where results were available). Results for the deep canyon were even better. The discrepancies with (28) for the larger values of η might be due to the slow convergence of that series solution for $|x/a| \geq 2$ and those values of η. The authors report than more terms of the series are needed when η and $|x/a|$ increase, and the results given here suggest that they did not take sufficiently many in the cases indicated.

It may be concluded that the method presented here is very good for semielliptical canyons of aspect ratio $b \geq 0.7$ and at least for frequencies $\eta \leq 1.5$ ($\eta/b \leq 1.5$ in deep cases) and probably also for somewhat larger values of η. By way of example, graphs of canyon shape, displacement amplitude and normalized displacement phase against normalized distance x/a for b = 0.7 and ϕ = 0°, 30°, 60°, 90° are given in Figs. 2 and 3 for shallow and deep semielliptical canyons respectively.

The validity of the method having been thus demonstrated, it has been applied to a trench with vertical walls $x = \pm a$ and curved floor with equation $r = a[\cos^2\theta+(d^2\cos^2\theta-\sin^2\theta)^2]^{-1/2}$, $|\tan\theta| > d$. In Figs. 4, 5 the form of this trench is shown for d=tan 30°, together with graphs of amplitude and phase of the surface motion w obtained for η = 0.5, 1.0 (N=25 and 36) respectively. Qualitatively similar results to those for semicylindrical and semielliptical canyons were observed. But it is of interest to note that, for waves propagating towards the right-hand side, the amplitude of the scattered wave near the left-hand wall can considerably exceed that of w^o, the sum of the incident and reflected plane waves. Finally, in this example no limitation on the topography slope is imposed as in methods involving the Rayleigh hypothesis (1, 5, 6, 7). Lack of accuracy of that method for steep slopes was reported in (4, p. 277).

ACKNOWLEDGEMENTS

We wish to thank C. Ruiz de Velasco who wrote the program used to produce the graphs and F.J. Sánchez Sesma for providing his program for the exact solution for the semi-cylindrical canyon. Also we thank F.J. Sánchez Sesma and E. Rosenblueth for a preprint of their paper.

BIBLIOGRAPHY

1. Aki, K. & Larner, K.L. 1970 Surface Motion of a Layered Medium Having an Irregular Interface Due to Incident Plane SH Waves, J. Geophys. Res. 75, 933-954.

2. Bates, R.H.T. 1975 Analytic Constraints on Electromagnetic Field Computations, IEEE Trans. Microwave Theory Tech. MTT - 23, 605-623.

3. Boore, D.M. 1972 Finite Difference Methods for Seismic Wave Propagation in Heterogeneous Materials, in Methods in Computational Physics, 11, 1-37.

4. Boore, D.M. 1972 A Note on the Effect of Simple Topography on Seismic SH Waves, Bull. Seism. Soc. Am. 62, 275-284.

5. Bouchon, M. 1973 Effect of Topography on Surface Motion, Bull. Seism. Soc. Am. 63, 615-632

6. Bouchon, M. & Aki, K. 1977 Discrete Wave-Number Representation of Seismic-Source Wave Fields, Bull. Seism. Soc. Am. 67, 259-277.

7. Bouchon, M. & Aki, K. 1977 Near-Field of a Seismic Source in a Layered Medium with Irregular Interfaces, Geophys. J. Roy. astr. Soc. 50, 669-684.

8. Burton, A.J. & Miller, G.F. 1971 The Application of Integral Equation Methods to the Numerical Solution of Some Exterior Boundary-Value Problems, Proc. Roy. Soc. Lond. A. 323, 201-210.

9. Gilbert, F. & Knopoff, L. 1960 Seismic Scattering from Topographic Irregularities, J. Geophys. Res. 65, 3437-3444.

10. Herrera, I. 1977 General Variational Principles Applicable to the Hybrid Element Method, Proc. Natl. Acad. Sci. USA 74, 2595-2597.

11. Herrera, I. 1977 Theory of Connectivity for Formally Symmetric Operators, Proc. Natl. Acad. Sci. USA 74, 4722-4725.

12. Herrera, I. 1978 Theory of Connectivity: A Systematic Formulation of Boundary Element Methods, First International Seminar on Boundary Element Methods, Southampton, England, July 5-7, 1978.

13. Herrera, I. & Sabina, F.J. 1978 Connectivity as an Alternative to Boundary Integral Equations. Construction of bases, Proc. Natl. Acad. Sci. USA 75, 2059-2063.

14. IBM 1970 System/360 Scientific Subroutine Package, Version III. 454 pp.

15. Kantorovich, L.V. & Krylov, V.I. 1964 Approximate Methods of Higher Analysis, N.Y.: Interscience.

16. McIvor, I. 1969 Two-Dimensional Scattering of a Plane Compressional Wave by Surface Imperfections, Bull. Seism. Soc. Am. 59, 1349-1364.

17. Millar, R.F. 1973 The Rayleigh Hypothesis and a Related Least-Squares Solution to Scattering Problems for Periodic Surfaces and Other Scatterers, Radio Science 8, 785-796.

18. Sabina, F.J. & Willis, J.R. 1975 Scattering of SH Waves by a Rough Half-Space of Arbitrary Slope, Geophys. J. Roy. astr. Soc. 42, 685-703.

19. Sabina, F.J. & Willis, J.R. 1977 Scattering of Rayleigh Waves by a Ridge, J. Geophys. 43, 401-419.

20. Sánchez Sesma, F.J. & Rosenblueth, E. 1978 Ground Motion at Canyons of Arbitrary Shape Under Incident SH Waves, Int. J. Earthquake Engng. Struct. Dyn. Submitted.

21. Sills, L.B. 1978 Scattering of Horizontally Polarized Shear Waves by Surface Irregularities, To be published.

22. Singh, S.K. & Sabina, F.J. 1977 Ground-Motion Amplification by Topographic Depressions for Incident P Wave Under Acoustic Approximation, Bull. Seism. Soc. Am. 67, 345-352.

23. Smith, W.D. 1974 A Nonreflecting Plane Boundary for Wave Propagation Problems, J. Comp. Phys. 15, 492-503.

24. Smith, W.D. 1975 The Application of Finite Element Analysis to Body Wave Propagation Problems, Geophys. J. Roy. astr. Soc. 42, 747-768.

25. Stroud, A.H. & Secrest, D. 1966 Gaussian Quadrature Formulas, N.Y.: Prentice-Hall.

26. Trifunac, M.D. 1973 Scattering of Plane SH Waves by a Semi-Cylindrical Canyon, Int. J. Earthquake Engng. Struct. Dyn. 1, 267-281.

27. Wong, H.L. & Jennings, P.C. 1975 Effects of Canyon Topography on Strong Ground Motion, Bull. Seism. Soc. Am. 65, 1239-1257.

28. Wong, H.L. & Trifunac, M.D. 1974 Scattering of Plane SH Waves by a Semi-Elliptical Canyon, Int. J. Earthquake Engng. Struct. Dyn. 3, 157-169.

29. Yasuura, K. & Ikuno, H. 1971 On the Modified Rayleigh Hypothesis and the Mode-Matching Method, International Symposium on Antennas and Propagation, Sendai, Japan, pp. 173-174, Institute of Electronics and Communication Engineers of Japan, Tokyo, Japan.

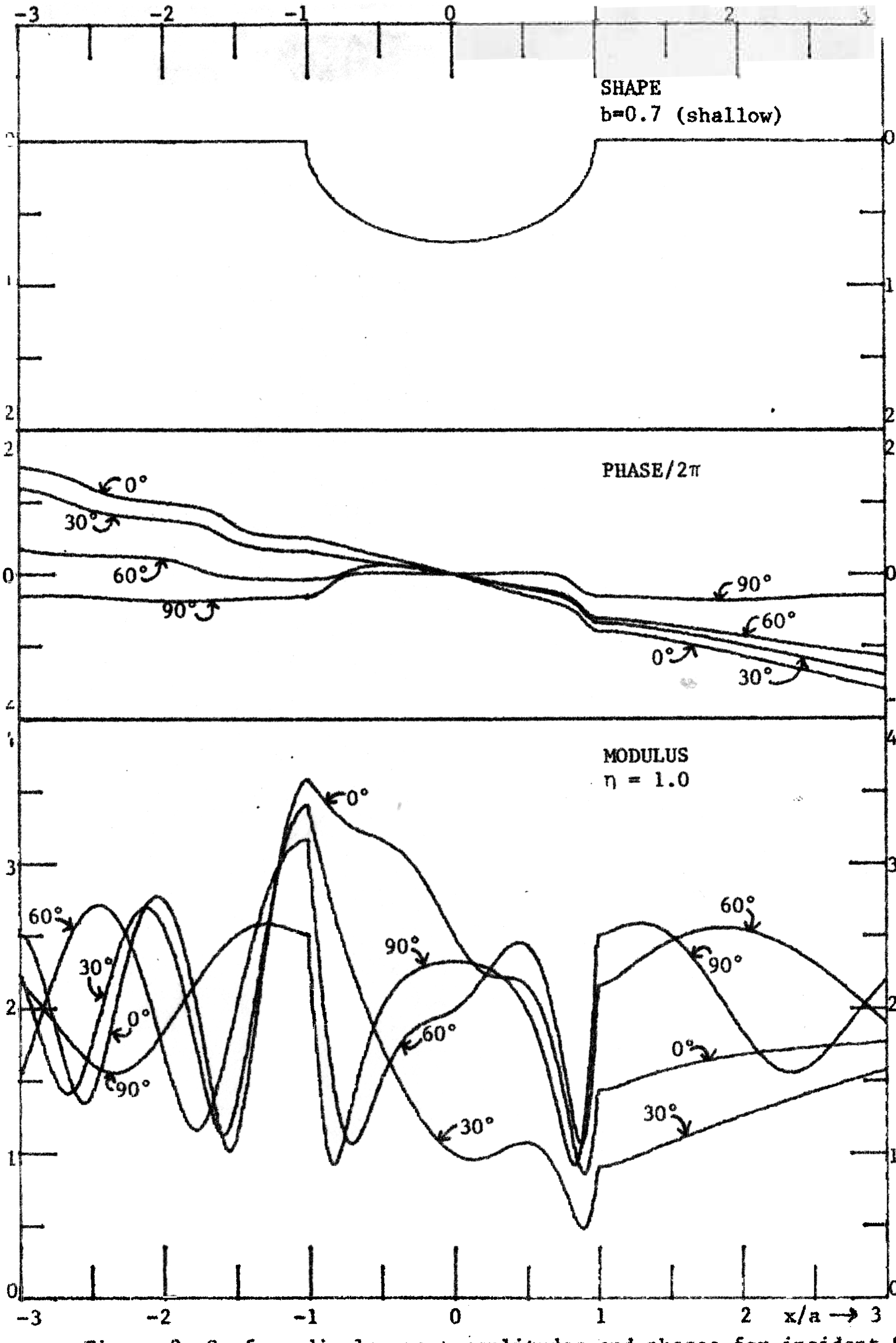

Figure 2. Surface displacement amplitudes and phases for incident SH waves and normalized frequency η=1.0. Shallow semiellipse of aspect radio b=0.7.

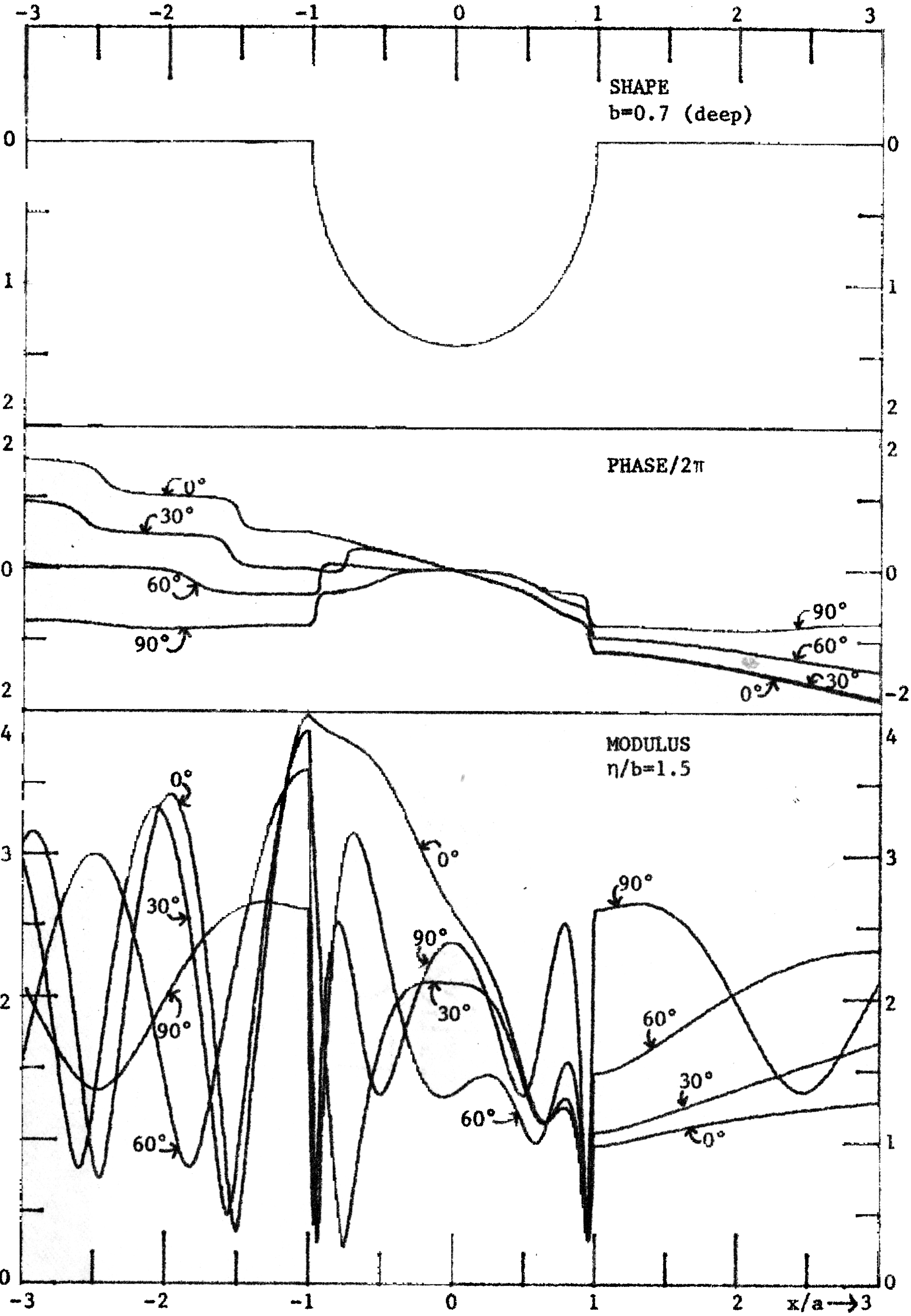

Figure 3. Surface displacement amplitudes and phases for incident SH waves and normalized frequency $\eta/b=1.5$. Deep semiellipse of aspect radio b=0.7.

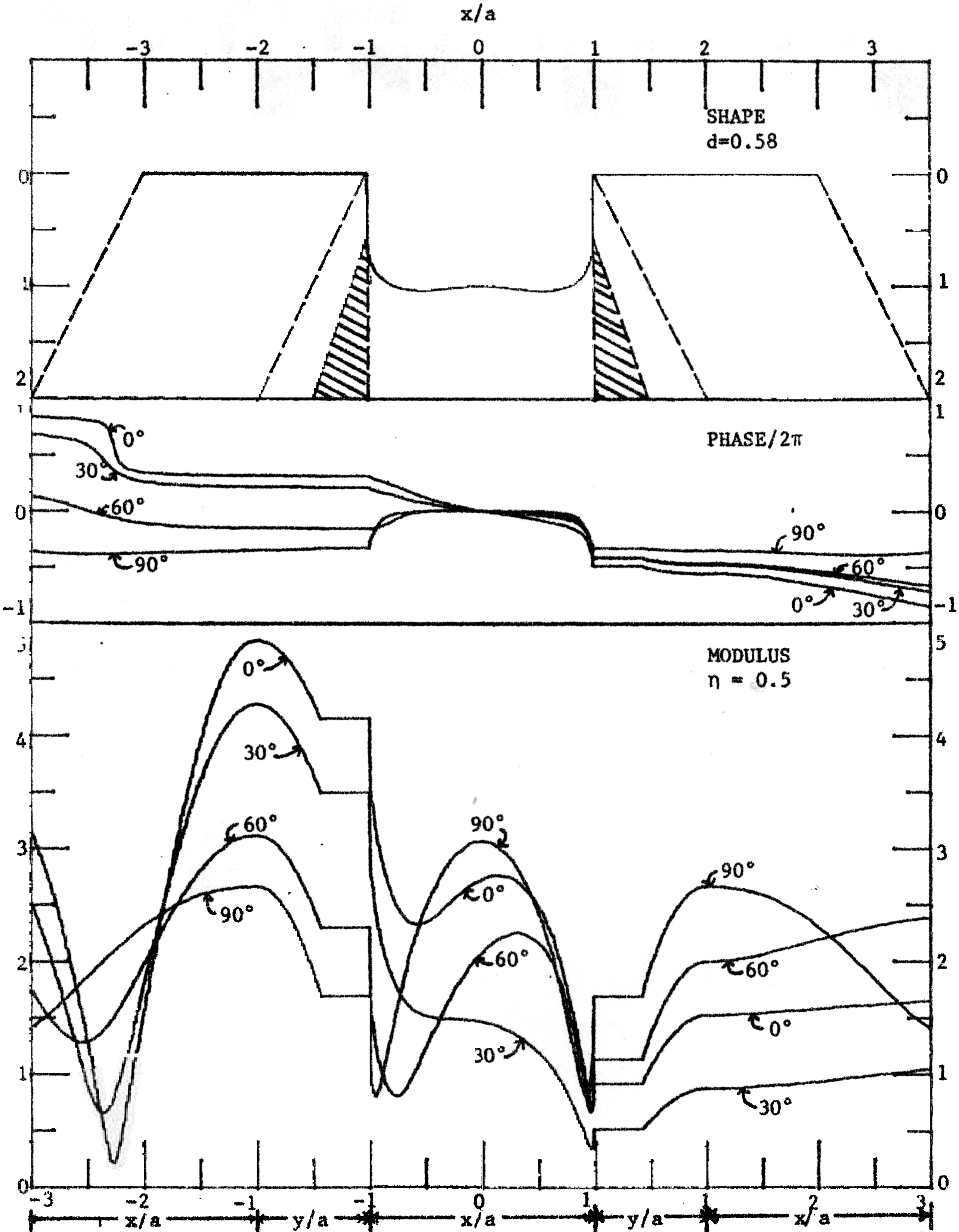

Figure 4. As Fig. 3 but for η=0.5 and a trench with vertical walls of depth d=0.58. The lower horizontal scale includes two intervals [-1,-1], [1,1] which represent distances y/a (along the vertical wall); the flat part corresponds to the wall-floor intersection point only.

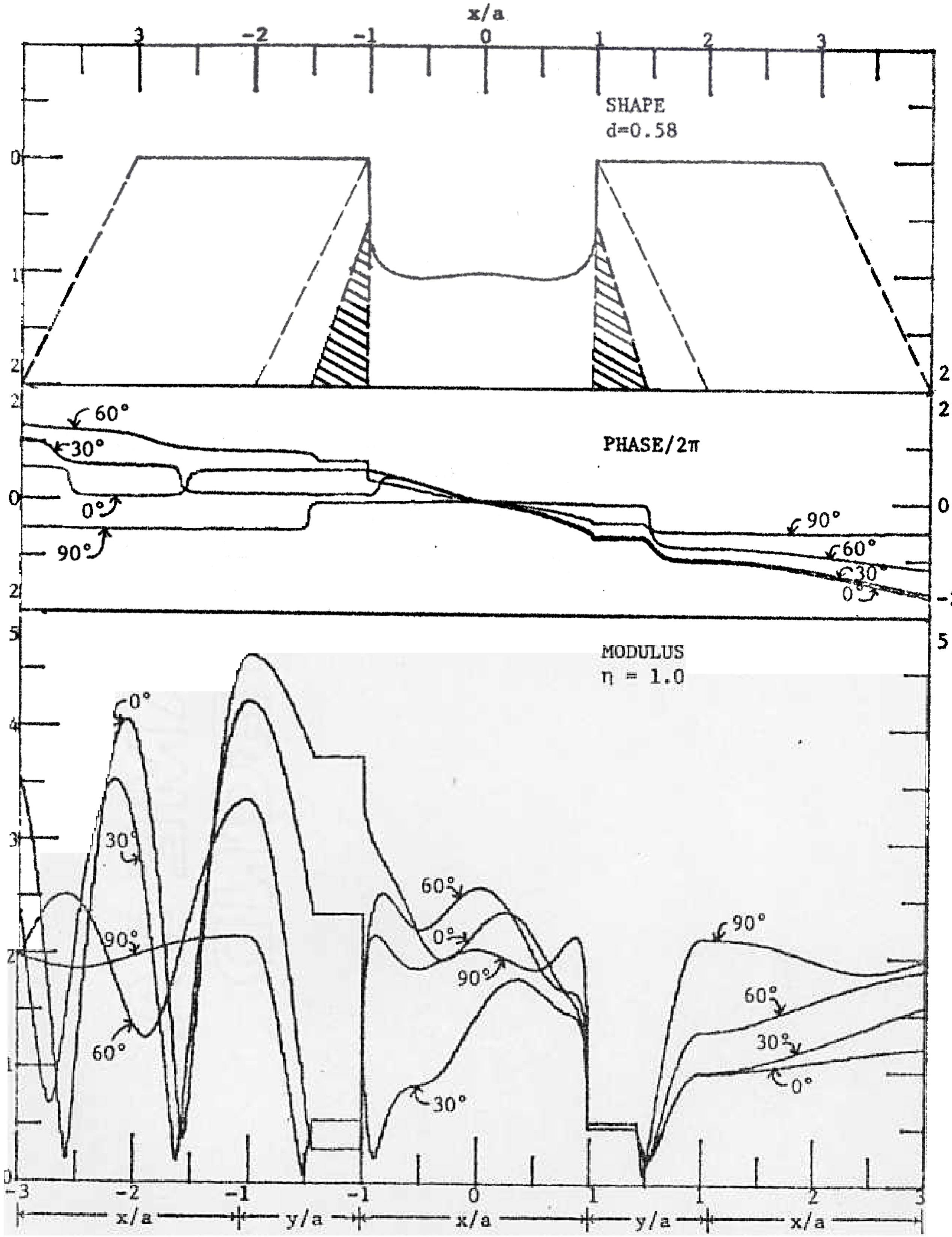

Figure 5. As Fig. 4 but for η=1.0.